

Combined NMR and Molecular Mechanics Study of the Isomers Formed in the Reaction of Dichloro(1,4-diazacycloheptane)platinum(II) with the Dinucleotide d(GpG)

Trevor W. Hambley,* Edwina C. H. Ling, and Barbara A. Messerle

School of Chemistry, University of Sydney, Sydney, NSW 2006, Australia

Received November 20, 1995[⊗]

The reaction of [Pt(hpip)Cl₂] (hpip = homopiperazine = 1,4-diazacycloheptane) with d(GpG) yields two apparently isomeric products, separable by HPLC. These have been characterized by a combination of 2D NMR and molecular mechanics modeling. NOESY correlations between the H8 protons show that both products are head-to-head isomers, and NOESY correlations between the d(GpG) dinucleotide and the diamine ligand show that the difference between the isomers lies in the orientation of the two and three carbon chains of the hpip ligand with respect to the heads (H8 protons) of the guanine bases. Molecular mechanics calculations yield total energies that are consistent with the observation of the two isomers in approximately equal amounts.

Introduction

It is believed that the anticancer activity of Pt(II) based drugs such as *cis*-DDP (*cis*-[Pt(NH₃)₂Cl₂]) is due to the formation of one or more bifunctional adducts.^{1–3} The most frequent adducts are intrastrand d(GpG) and d(ApG),^{4–8} and there is substantial evidence that one or both of them may be responsible for the anticancer activity.^{3,9–13} However, there is also evidence implicating the lower frequency GG interstrand adducts.^{14–16} We have designed a series of complexes to interact stereospecifically with DNA and so give rise to an adduct profile different from that formed by *cis*-DDP.^{17–21} The long-term aim of these studies is to investigate any correlation between anticancer

activity and adduct profile and so contribute to an understanding of the mechanism of action of Pt anticancer drugs.

[Pt(hpip)Cl₂] (hpip = homopiperazine = 1,4-diazacycloheptane) was designed to be readily able to form interstrand adducts but to be less likely to form intrastrand adducts than *cis*-DDP.²¹ In a preliminary report we showed that these design goals were achieved, with [Pt(hpip)Cl₂] forming interstrand adducts at approximately the same level as *cis*-DDP but forming intrastrand adducts, on salmon sperm DNA, at a substantially lower level.²¹ As part of the study of the intrastrand d(GpG) adducts formed by [Pt(hpip)Cl₂], we prepared the complex [Pt(hpip)d(GpG)]¹ and found by HPLC analysis that two isomers were formed in approximately equal amounts.^{21,22} HPLC analysis of the adducts formed in the reaction between [Pt(hpip)Cl₂] and salmon sperm DNA also revealed two intrastrand d(GpG) isomers but in unequal proportions.²² This latter result indicated that the reaction between [Pt(hpip)Cl₂] and duplex DNA is stereoselective, and, therefore, it became important to characterize the two isomers. It was considered probable that the origin of the isomerism related to the relative dispositions of the dinucleotide and the diamine ligand. Kiser *et al.* have recently shown that crosspeaks in 2D NMR spectra between nucleotide and diamine ligand protons are particularly useful for determining which isomers are present.²³ Following a similar approach we have carried out a 1D and 2D NMR study to characterize the two isomers. To aid in the interpretation of the 2D NMR spectra and to aid in assigning the isomers we have also carried out a molecular mechanics analysis of the various isomers and describe the results herein.

Experimental Section

Materials. The sodium salt of d(GpG) was purchased from Sigma. [Pt(hpip)Cl₂] was synthesized as described elsewhere.²¹

Preparation of the [Pt(hpip)d(GpG)]^{*} Isomers. [Note: Asterisk indicates that we have not assigned a charge to [Pt(hpip)d(GpG)] because its charge is pH dependent.] Large quantities of the two [Pt(hpip)d(GpG)]^{*} isomers were prepared for ¹H NMR spectroscopy as follows. [Pt(hpip)Cl₂] in 0.02 M NaClO₄ (1.37 mM, 3.7 mL) was reacted with 1 equiv of d(GpG) (3.13 mg) in 0.02 M NaClO₄, pH 5.5, for 24 h at 37 °C. The mixture was concentrated to approximately 1.5 mL by freeze-drying, and 200 μL aliquots were loaded onto a Waters

[⊗] Abstract published in *Advance ACS Abstracts*, July 1, 1996.

- (1) Pinto, A. L.; Lippard, S. J. *Biochem. Biophys. Acta* **1985**, *780*, 167–180.
- (2) van der Veer, J. L.; Reedijk, J. *Chem. Brit.* **1988**, *24*, 775–780.
- (3) Sheibani, N.; Jennerwein, M. M.; Eastman, A. *Biochemistry* **1989**, *28*, 3120–3124.
- (4) Fichtinger-Schepman, A. M. J.; Lohman, P. H. M.; Reedijk, J. *Nucleic Acids Res.* **1982**, *10*, 5345–5356.
- (5) Eastman, A. *Biochemistry* **1983**, *22*, 3927–3933.
- (6) Fichtinger-Schepman, A. M. J.; van der Veer, J. L.; den Hartog, J. H. J.; Lohman, P. H. M.; Reedijk, J. *Biochemistry* **1985**, *24*, 707–713.
- (7) Eastman, A. *Biochemistry* **1985**, *24*, 5027–5032, **1986**, *25*, 3912–3915.
- (8) Pinto, A. L.; Naser, N. J.; Essigmann, J. M.; Lippard, S. J. *J. Am. Chem. Soc.* **1986**, *108*, 7405–7407.
- (9) Corda, Y.; Job, C.; Anin, M. F.; Leng, M.; Job, D. *Biochemistry* **1991**, *30*, 222–230.
- (10) Comess, K. M.; Burstyn, J. N.; Essigmann, J. M.; Lippard, S. J. *Biochemistry* **1992**, *31*, 3975–3990.
- (11) Corda, Y.; Anin, M. F.; Leng, M.; Job, D. *Biochemistry* **1992**, *31*, 1904–1908.
- (12) Naser, L. J.; Pinto, A. L.; Lippard, S. J.; Essigmann, J. M. *Biochemistry* **1988**, *27*, 4357–4367.
- (13) Bradley, L. J. N.; Yarema, K. J.; Lippard, S. J.; Essigmann, J. M. *Biochemistry* **1993**, *32*, 982–988.
- (14) Jones, J. C.; Zhen, W.; Reed, E.; Parker, R. J.; Sancar, A.; Bohr, V. A. *J. Biol. Chem.* **1991**, *266*, 7101–7107.
- (15) Zhen, W.; Link, C. J., Jr.; O'Connor, P. M.; Reed, E.; Parker, R.; Howell, S. B.; Bohr, V. A. *Mol. Cell. Biol.* **1992**, *12*, 3689–3698.
- (16) Corda, Y.; Job, C.; Anin, M. F.; Leng, M.; Job, D. *Biochemistry* **1993**, *32*, 8582–8588.
- (17) Hambley, T. W. *Inorg. Chem.* **1991**, *30*, 937–942.
- (18) Hambley, T. W. *Comments Inorg. Chem.* **1992**, *14*, 1–26.
- (19) Vickery, K.; Bonin, A. M.; Fenton, R. R.; O'Mara, S.; Russell, P. J.; Webster L. K.; Hambley, T. W. *J. Med. Chem.* **1993**, *36*, 3663–3668.
- (20) Ling, E. C. L.; Allen, G. W.; Hambley, T. W. *J. Chem. Soc., Dalton Trans.* **1993**, 3705–3710.
- (21) Ling, E. C. L.; Allen, G. W.; Hambley, T. W. *J. Am. Chem. Soc.* **1994**, *116*, 2673–2674.

(22) Ling, E. C. L.; Hambley, T. W. Manuscript in preparation.

(23) Kiser, D.; Intini, F. P.; Xu, Y.; Natile, G.; Marzilli, L. G. *Inorg. Chem.* **1994**, *34*, 4149–4158.

Prep Nova-Pak HR C18 preparative column (6 μm , 60 \AA particle size, 25 \times 100 mm) enclosed in a Waters 25 \times 10 RCM cartridge. The elution was performed with methanol in ammonium acetate buffer at 7 mL min^{-1} . HPLC fractions were collected every 25 s and were pooled according to the chromatograms. White solids were obtained when the solutions of band I and band II were lyophilized. The bands were separately resuspended in water and freeze-dried several times to remove all traces of ammonium acetate. Minor impurities, including residual methanol and ammonium acetate buffer, were observed in the NMR spectra, but these did not interfere with the analyses.

NMR Spectroscopy. Solutions of each of the isomers (2 mM) were prepared in dimethyl- d_6 sulfoxide (Sigma). NMR spectra were recorded on Bruker AMX400 and AMX600 spectrometers at 303 K. Spectra were recorded over spectral widths of 5000 Hz with quadrature detection employed throughout. Two-dimensional spectra were acquired in the phase-sensitive mode using time-proportional phase incrementation.²⁴ Data sets resulting from 512 increments of t_1 were acquired and zero filled to 1024 points, with each free induction decay composed of 2048 data points. Typically, 32 transients were recorded for each increment of t_1 with a recycle delay of 1.6 s. Double quantum filtered COSY²⁵ spectra were acquired using the standard pulse sequence. NOESY^{26–28} spectra were recorded with mixing times (τ_m) equal to 300 and 600 ms with a recycle delay of 1.6 s. Data was subjected to shifted sine-bell weighting functions in f1 and f2 of $\pi/2$ and were base line corrected where required using Bruker software on an X32 data station. Crosspeak intensities were determined by integration using Bruker software.

Molecular Mechanics Modeling. Models of the possible isomers of the bifunctional $[\text{Pt}(\text{hpi})\text{d}(\text{GpG})]^+$ adduct were generated using molecular mechanics calculations. The HyperChem program²⁹ was used to construct monofunctional starting structures where a $[\text{Pt}(\text{hpi})\text{Cl}]^+$ moiety was attached to one N7 guanine atom of a d(GpG) dinucleotide. The energies of these monofunctional structures were then minimized using MOMECC-91³⁰ and a force field described previously.¹⁷ Bifunctional models were generated using constraints to reduce the distance between the platinum atom and the second N7 guanine atom to the required bonding distance. The constraint was then released and the strain energies of the resultant bifunctional models were minimized until all shifts in positional coordinates were less than or equal to 0.001 \AA . Models of the possible head-to-head isomers were also constructed using the crystal structure of $[\text{Pt}(\text{NH}_3)_2\text{d}(\text{pGpG})]^{31–33}$ as a starting point. Models of the head-to-tail isomers were generated by using constraints to enforce rotation of the nucleobases with respect to the attached sugar rings from the *anti* configuration to *syn* configuration. Attempts were made to generate *syn, syn* isomers in the same way, but in all cases, energy minimization resulted in reorganization to a *syn, anti* or *anti, syn* isomer.

Results and Discussion

Two bands (I and II) were observed at 10.0 and 11.1 min in the HPLC analysis of the reaction products formed between $[\text{Pt}(\text{hpi})\text{Cl}_2]$ and d(GpG).²² These were studied separately using 1D and 2D ^1H NMR spectroscopy, and the resultant 1D ^1H NMR spectra and 2D COSY spectra are illustrated in Figures

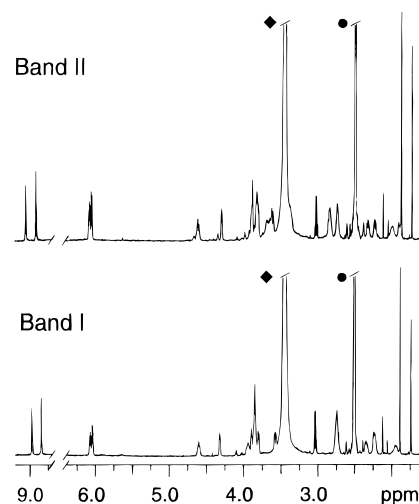


Figure 1. 1D ^1H NMR spectra (600 MHz, 303 K, solvent $\text{C}_2\text{D}_6\text{SO}$) of the two species obtained from the reaction between $[\text{Pt}(\text{hpi})\text{Cl}_2]$ and d(GpG) (\blacklozenge , CH_3OH ; \bullet , residual $\text{C}_2\text{D}_6\text{SO}$).

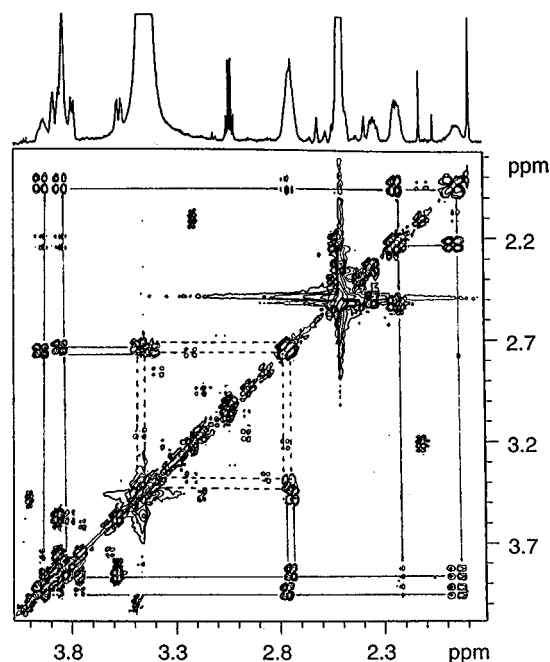


Figure 2. Portion of the COSY spectrum for band I recorded at 600 MHz, 303 K. Connectivities between the resonances due to the protons of the two- and three-carbon chains of hpi are shown, where - - - represents a two-carbon chain and — represents a three-carbon chain.

1–3. For each band, the bulk of the resonances in the 1D spectrum were assigned with the aid of the corresponding COSY spectrum. The hpi ligand NH protons (Figure 4) were assigned using the NOESY spectra, as the ligand NH protons are necessarily close to other protons on the amine ligand. Similarly, the nucleotide protons H8a and H8b (Figure 4) were assigned using the NOESY spectra, as proton H8 is necessarily close to proton H1' of the sugar ring within each nucleotide subunit. Stereospecific assignments were not made, with the exception of the H2' and H2'' protons on the sugar rings and some protons on the hpi ligand. A summary of the chemical shifts is presented in Tables 1 and 2.

The chemical shifts are all similar to those observed in closely related complexes.^{34–38} The H8 signals are further downfield

- (24) Marion, D.; Wütrich, K. *Biochem. Biophys. Res. Commun.* **1983**, *113*, 967–974.
 (25) Piantini, U.; Sorenson, O.; Ernst, R. R. *J. Am. Chem. Soc.* **1982**, *104*, 6800–6801.
 (26) Jeener, J.; Meier, B. H.; Bachmann, P.; Ernst, R. R. *J. Chem. Phys.* **1979**, *71*, 4546–4553.
 (27) Kumar, A.; Ernst, R. R.; Wütrich, K. *Biochem. Biophys. Res. Commun.* **1980**, *95*, 1–16.
 (28) Macura, A.; Ernst, R. R. *Mol. Phys.* **1980**, *41*, 95–117.
 (29) HYPERCHEM, Hypercube Inc., Ontario, Canada.
 (30) Hambley, T. W. MOMECC-91, Programme for Strain Energy Minimization; University of Sydney, Australia, 1991.
 (31) Sherman, S. E.; Gibson, D.; Wang, A. H. J.; Lippard, S. J. *Science* **1985**, *230*, 412–417.
 (32) Sherman, S. E.; Gibson, D.; Wang, A. H. J.; Lippard, S. J. *J. Am. Chem. Soc.* **1988**, *110*, 7368–7381.
 (33) Coll, M.; Sherman, S. E.; Gibson, D.; Lippard, S. J.; Wang, A. H. J. *J. Biomol. Struct. Dyn.* **1990**, *8*, 315–330.

- (34) den Hartog, J. H. J.; Altona, C.; Chottard, J. C.; Girault, J. P.; Lallemand, J. Y.; de Leeuw, F. A. A. M.; Marcelis, A. T. M.; Reedijk, J. *Nucleic Acids Res.* **1982**, *10*, 4715–4730.

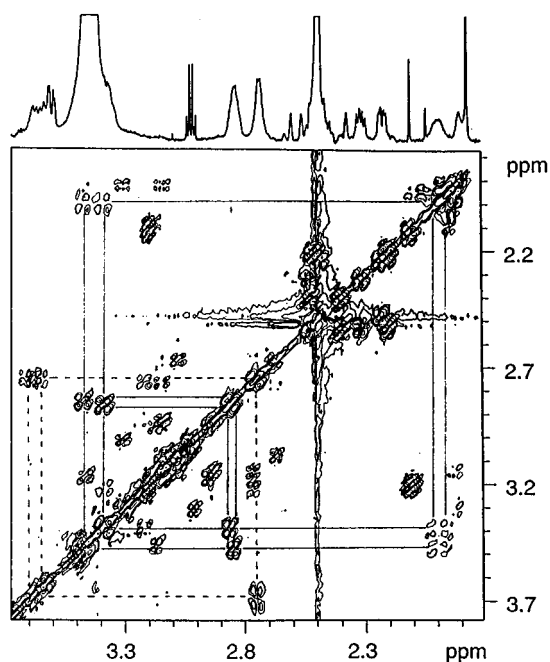


Figure 3. Portion of COSY spectrum for band II recorded at 600 MHz, 303 K. Connectivities between the resonances due to the protons of the two- and three-carbon chains of hpip are shown, where - - - represents a two-carbon chain and — represents a three-carbon chain.

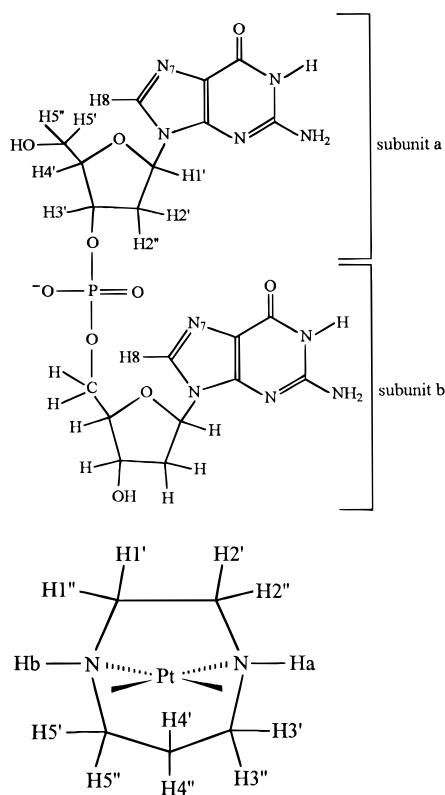


Figure 4. Labeling used for the hpip and d(GpG) protons.

shifted than those in other complexes of d(GpG), and unusually, the 5'-H8 signal is further downfield than is the 3'-H8 signal.

- (35) den Hartog, J. H. J.; Altona, C.; van der Marel, G. A.; Reedijk, J. *Eur. J. Biochem.* **1985**, *147*, 371–379.
 (36) van der Veer, J. L.; van der Marel, G. A.; van den Elst, H.; Reedijk, J. *Inorg. Chem.* **1987**, *26*, 2272–2275.
 (37) Girault, J. P.; Chottard, G.; Lallemand, J. Y.; Chottard, J. C. *Biochemistry* **1982**, *21*, 1352–1356.
 (38) Kozelka, J.; Fouchet, M.-H.; Chottard, J.-C. *Eur. J. Biochem.* **1992**, *205*, 895–906.

Table 1. Chemical Shifts Assigned to the hpip Ligand

proton	chemical shift (ppm)		proton	chemical shift (ppm)	
	band I	band II		band I	band II
H1'	2.79	2.80	H4'	1.99	1.96
H1''	3.52	3.76	H4''	2.29	2.05
H2'	2.82	2.80	H5'	2.79	2.91
H2''	3.46	3.71	H5''	3.91	3.51
H3'	2.81	2.91	NHa	7.76	7.26
H3''	4.00	3.44	NHb	7.68	7.32

Table 2. Chemical Shifts Assigned to d(GpG)

proton	chem shift (ppm)		proton	chem shift (ppm)	
	band I	band II		band I	band II
H1'a	6.10	6.15	H1'b	6.13	6.14
H2'a	2.39	2.26	H2'b	2.29	2.57
H2''a	2.55	2.57	H2''b	2.57	2.38
H3'a	4.66	4.41	H3'b	4.38	4.69
H4'a	3.85	3.99	H4'b	3.93	3.87
H5'a	3.65	3.82	H5'b	3.81	3.67
H5''a	3.91	3.91	H5''b	3.91	3.95
H8a	9.02	9.09	H8b	8.88	8.95

In these respects, the H8 signals have more in common with those seen in complexes of d(ApG).³⁸ Kozelka *et al.* have shown that the ring current effect of one guanine influences the shift of the H8 of the other guanine, and this is related to the conformation of the dinucleotide. The hpip ligand is conformationally rigid, and interactions, such as hydrogen bonds, between it and the dinucleotide can influence the orientation of the guanine bases.³⁹ Therefore, it is not surprising that unusual H8 shifts are observed in these [Pt(hpip)d(GpG)]⁺ complexes.

The similarity of the NMR spectra of the two bands obtained by HPLC analysis of the [Pt(hpip)d(GpG)]⁺ preparation is consistent with these species being isomers of the adduct, most probably with the platinum atom coordinated in each case to the two guanine N7 atoms of the dinucleotide. Because of the unsymmetrical nature of the hpip ligand, d(GpG) can coordinate in two ways, with the “heads” (H8 atoms) of the nucleobases disposed toward the two carbon chain of the hpip or toward the three carbon chain. Interconversion between these isomers cannot take place without breaking and re-forming of coordinate (Pt–N) bonds. Additionally, on the basis of previous studies with platinated mono-,^{23,39–42} di-,³⁴ tri-,^{35,36} and tetranucleotides,⁴³ it was postulated that rotation about the Pt–N7(G) bonds might be restricted by the rigid hpip ligand. The [Pt(hpip)d(GpG)]⁺ adduct might, therefore, adopt any of six potentially noninterconverting isomers, two head-to-head isomers, one with the two carbon chain of hpip lying on the same side of the coordination plane as the H8 atoms of the purine bases (HTH/2), and the other with the three carbon chain of hpip lying on the same side of the coordination plane as the H8 atoms of the purine bases (HTH/3). Similarly, there are four head-to-tail isomers, one *anti*, *syn* and *syn*, *anti* pair, each with the H8 of the 5' base on the same side of the coordination plane as the two carbon chain (HTT/2a and HTT/2b) and a second pair with the H8 of the 5' base on the same side of the coordination plane as the three carbon chain (HTT/3a and HTT/3b). In order to facilitate the interpretation of the crosspeaks in the 2D NMR spectra, these six isomers of [Pt(hpip)d(GpG)]⁺

(39) Hambley, T. W. *Inorg. Chem.* **1988**, *27*, 1073–1077.

(40) Reilly, M. D.; Marzilli, L. G. *J. Am. Chem. Soc.* **1986**, *108*, 6785–6793.

(41) Xu, Y.; Natile, G.; Intini, F. P.; Marzilli, L. G. *J. Am. Chem. Soc.* **1990**, *112*, 8177–8179.

(42) Berners-Price, S. J.; Frey, U.; Ranford, J. D.; Sadler, P. J. *J. Am. Chem. Soc.* **1993**, *115*, 8649–8659.

(43) Neumann, J. M.; Tran-Dinh, S.; Girault, J. P.; Chottard, J. C.; Huynh-Dinh, T.; Igolen, J. *Eur. J. Biochem.* **1984**, *141*, 465–472.

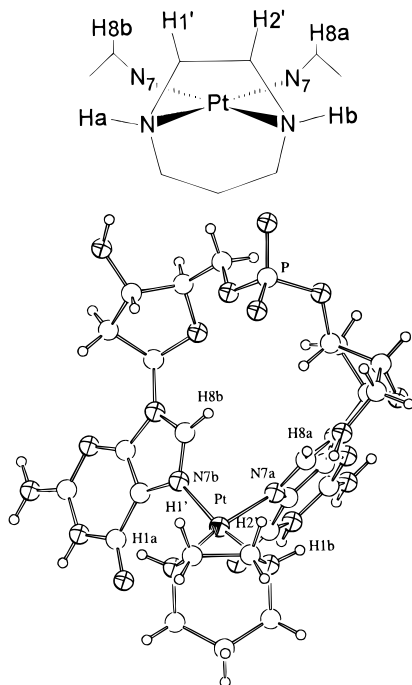


Figure 5. Molecular model and schematic diagram of the head-to-head isomer of $[\text{Pt}(\text{hpip})\text{d}(\text{GpG})]$, where the two-carbon ring of hpip lies on the same side of the coordination plane as the H8 atoms (HTH/2).

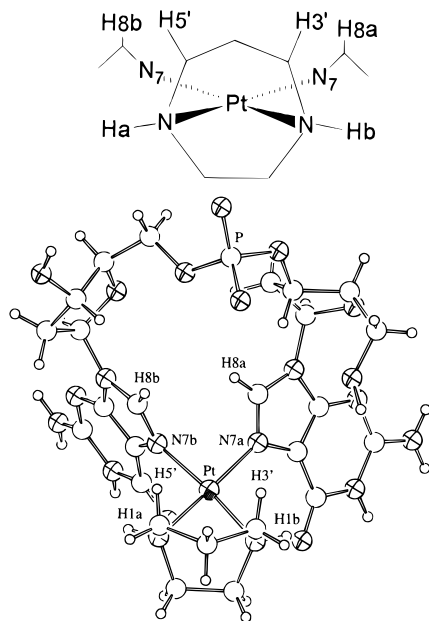


Figure 6. Molecular model and schematic diagram of the head-to-head isomer of $[\text{Pt}(\text{hpip})\text{d}(\text{GpG})]$, where the three-carbon ring of hpip lies on the same side of the coordination plane as the H8 atoms (HTH/3).

were modeled using molecular mechanics calculations, and the results are discussed below. The resultant models of the two head-to-head isomers are illustrated in Figures 5 and 6, and the closest proton–proton interactions between the hpip and dinucleotide ligands for the six models are listed in Table 3.

It is apparent from Table 3 that a number of the interligand $\text{H}\cdots\text{H}$ distances differ significantly between the various models. Thus, the NOESY spectra, in combination with the models, can be used to determine which of the isomers correspond to bands I and II. Key NOESY correlations for bands I and II are listed in Table 4. In most respects the NOESY correlations of the two bands are similar, but there are also significant differences.

Table 3. Comparison of the Interactions within the Conformational Isomers of $[\text{Pt}(\text{hpip})\text{d}(\text{GpG})]$

interactn	distance (Å)					
	HTH/2	HTH/3	HTT/2a	HTT/2b	HTT/3a	HTT/3b
H8a \cdots H8b	3.1	2.5	5.1	5.1	4.4	5.1
H8a \cdots NHb	2.7	4.4	3.8	3.7	4.0	3.9
H8b \cdots NHa	4.5	3.7	4.2	3.6	4.1	3.4
H8a \cdots H2'	3.3	5.9	4.1	4.1	5.7	5.7
H8b \cdots H1'	4.7	5.6	5.9	5.5	4.4	3.9
H8a \cdots H3'	4.6	3.9	5.3	5.2	3.5	3.3
H8b \cdots H5'	6.6	3.2	3.7	3.1	5.6	5.0

Table 4. Relative Intensities of Key NOESY Correlations in the Spectrum for Bands I ($\tau_m = 300$ ms) and II ($\tau_m = 600$ ms)

interactn	rel intens of NOESY crosspeak	interactn	rel intens of NOESY crosspeak
H8a \cdots H8b	3370	H8a \cdots H2'	122
H8a \cdots NHb	151	geminal pairs	12 000, 16 000, 15 000
H8b \cdots NHa	277		
		Band II	
H8a \cdots H8b	7960	H8a \cdots H3'	260
H8a \cdots NHb	189	H8b \cdots H5'	250
H8b \cdots NHa	176	geminal pairs	15 300, 10 500

Medium-strength NOESY correlations were observed between nucleotide protons H8a and H8b (Table 4). As the intensities of these crosspeaks were the same order of magnitude as the NOESY correlations observed between geminal pairs of protons, it was concluded that in bands I and II the nucleotide protons H8a and H8b must be close together (approximately 2.4–3 Å). As protons H8a and H8b are 2.5–3.1 Å apart in the head-to-head models and 4.4 Å or more apart in the head-to-tail models (Table 3), the medium strength H8a \cdots H8b crosspeaks are consistent with both bands being head-to-head conformational isomers of the $[\text{Pt}(\text{hpip})\text{d}(\text{GpG})]^*$ adduct. Furthermore, as NOE intensity is proportional to the distance r raised to the inverse sixth power (r^{-6}),⁴⁴ the intensity of the crosspeaks would be expected to be at least 2 orders of magnitude weaker if protons H8a and H8b were 4 Å apart as predicted for the head-to-tail isomers. It has to be said that the molecular mechanics generated model of each isomer represents one possible minimum (conformation) on what is undoubtedly a complex potential energy surface. Indeed we observed a number of different conformations, the major variant being the presence or lack of hydrogen bonds between H(amine) and O6(guanine) atoms. The data presented in Table 3 derive from models without such hydrogen bonds for reasons outlined below. Additionally, molecular mechanics models represent a static view of one possible conformation of each isomer, whereas NMR spectra represent a time-averaged view of an isomer in constant motion. However, it is difficult to envisage variations of the head-to-tail isomers in which the H8a and H8b protons were substantially closer than 4 Å.

A second set of weak NOESY correlations between the nucleotide H8 protons and the corresponding hpip ligand NH protons (Table 4) are also consistent with both of the bands being head-to-head isomers but cannot be used to rule out head-to-tail isomers. These separations vary significantly between different molecular mechanics models depending on the presence or absence of intramolecular O6 \cdots H(N) hydrogen bonds.

These results, and in particular the strong H8 \cdots H8 crosspeaks, provide strong evidence that bands I and II are both head-to-head conformational isomers of the $[\text{Pt}(\text{hpip})\text{d}(\text{GpG})]^*$ adduct.

(44) Neuhau, D.; Williamson, M. P. *The Nuclear Overhauser Effect in Structural and Conformational Analysis*, 1st ed.; VCH Publishers: New York, 1989.

Table 5. Comparison of the Strain Energies for the Conformational Isomers of [Pt(hpip)d(GpG)]^a

energy component	energy (kJ mol ⁻¹)					
	HTH/2	HTH/3	HTT/2a	HTT/2b	HTT/3a	HTT/3b
bond deformation	5.2	5.3	5.1	5.5	5.0	5.6
nonbonded interactn	31.1	29.2	14.6	5.7	16.0	5.2
valence angle deformation	32.3	35.4	31.3	36.8	30.5	36.8
torsion angle deformation	48.5	44.7	54.9	48.6	55.4	48.4
electrostatic interactn	-268.5	-264.7	-268.3	-256.2	-267.8	-256.1
out of plane deformation	1.1	0.2	1.2	0.5	1.1	0.5
tot. strain	-150.3	-149.9	-161.2	-159.0	-159.7	-159.7

This is not an unexpected result since previous studies on Pt complexes of d(GpG) have revealed only head-to-head isomers.^{31–36,43,45}

Differences between the NOESY correlations of the two bands were also used to establish the orientation of the hpip ligand with respect to the dinucleotide in each case. Although the NOESY correlations between the nucleotide H8 protons and the hpip ligand protons were weak, the assignments were made on the basis that NOE crosspeaks are not normally detected when protons are further apart than 4.0–4.5 Å. In the NOESY spectrum for band II, weak crosspeaks were detected between nucleotide proton H8a and hpip ligand proton H3' and between nucleotide proton H8b and hpip ligand proton H5' (Table 4). No other crosspeaks were observed between the hpip ligand and the dinucleotide. In the molecular mechanics generated models, distances between the nucleotide H8 protons and protons on the three carbon chain of hpip are, as expected, shorter when the three carbon chain of hpip lies on the same side of the coordination plane as the H8 atoms (Table 3). The closest H8a...H3' and H8b...H5' distances are respectively 4.6 and 6.6 Å for HTH/2 and 3.9 and 3.2 Å for HTH/3. Thus, it can be concluded that, in band II of the [Pt(hpip)d(GpG)]^a adduct, the three-carbon chain of hpip lies on the same side of the coordination plane as the H8 atoms (Figure 6). Similarly, the weak NOESY crosspeak between the nucleotide proton H8a and the hpip ligand proton H2' (refer to Table 4) reveal that, in band I, the two-carbon chain of hpip lies on the same side of the coordination plane as the H8 atoms (Figure 5). The predicted distances between the nucleotide H8 protons and protons on the two carbon chain of hpip are shorter when the two carbon chain of hpip lies on the same side of the coordination plane as the H8 atoms (Table 3). The H8a...H2' distance is 4.4 Å for HTH/2 and 5.9 Å for HTH/3. In some cases these weak crosspeaks do not follow the intensity order expected based on the predicted separation, but we stress again that other slightly different conformations are possible and probably contribute. Taken together, all of the evidence is clearly consistent with band I corresponding to HTH/2 and band II to HTH/3.

The relative strain energies of the six isomers are listed together in Table 5. The head-to-head isomers of the [Pt(hpip)d(GpG)]^a adduct have strain energies about 10 kJ mol⁻¹ higher than do the head-to-tail isomers, which is unexpected given that only head-to-head isomers are observed for [Pt(hpip)d(GpG)]^a and for other Pt complexes containing the d(GpG) dinucleotide.^{31–36,43,45} The lower strain energy of the head-to-tail isomers is principally due to smaller contributions from nonbonded interactions. Again, we would not rule out the possibility that there are other, lower energy, conformational

forms of the head-to-head isomers that we have not identified. It is also possible that hydrogen bonding is responsible for the stabilization of the head-to-head isomers, but it may simply be that the molecular mechanics models are not accurate enough to reliably predict the strain energies of such molecules. The difference between the relative strain energies of the two head-to-head species is small and of marginal significance, in accord with the two isomers being observed in equal proportions.

In most respects the geometries of the two head-to-head isomers accord well with the distances that can be inferred from the strength of the crosspeaks in the 2D NMR spectra of bands I and II. There are some minor exceptions; however, as we have pointed out above, there are undoubtedly many other conformations with similar energies. The presence or absence of hydrogen bonds between the H(amine) atoms and O6-(guanine) atoms will have an unusually strong influence on the conformation because of the rigidity of the hpip ligand. We have presented the results of models without such hydrogen bonds because, although they are sometimes observed in the solid state, we believe that in solution the additional opportunities for hydrogen bonding with the solvent would lead to low populations of the intramolecularly hydrogen-bonded conformations. We have also investigated models with intramolecular hydrogen bonds, and some of these are more consistent with the crosspeaks observed in the NMR spectra. However, given the myriad of conformations available, we consider it inappropriate to make use of such selective comparisons and, instead, have presented only the results for the conformations of lowest strain energy.

The conformational geometry of the d(GpG) dinucleotide differs slightly between HTH/2 and HTH/3 with the variation being similar to that observed in the crystal structure of [Pt(NH₃)₂d(pGpG)].^{31–33} The angles between the coordination plane and the planes through the guanine bases are as follows: HTH/2, 109.7° (5') and 52.4° (3'); HTH/3, 127.2° (5') and 90.3° (3'); [Pt(NH₃)₂d(pGpG)], 111.1–76.8° (5') and 95.4–57.8° (3').^{31–33} The H8...H8 separations (HTH/2, 3.1 Å, HTH/3, 2.5 Å) are also significantly different (consistent with the NOESY correlations) with again that for HTH/3 being more like the separation calculated for the same atoms in the aforementioned crystal structure (*ca.* 2.65 Å).^{31–33} These differences between the otherwise similar conformations appear to be due to interactions between the H(amine) atoms and the dinucleotide. The unsymmetrical geometry of the hpip ligand results in these H atoms being disposed above and below the coordination plane in HTH/2 and HTH/3, respectively, and so they interact differently with the dinucleotide. Initially, we were surprised that two isomers differing only with respect to the orientation of the hpip ligand were so readily separable by HPLC. However, it would appear that the orientation of the hpip ligand has an influence on the conformation of the dinucleotide, providing a rationalization for the chromatographic separation.

Conclusions

The NMR spectra of the two bands obtained by HPLC analysis of the products obtained from the reaction of [Pt(hpip)Cl₂] with d(GpG) provide strong evidence that both bands are predominantly head-to-head isomers, one with the two carbon chain of the hpip ligand disposed toward the "heads" (H8 ends) of the guanine bases and the other with the three-carbon chain disposed in that direction. The molecular mechanics results are in accord with the two isomers being observed in equal proportions.

When [Pt(hpip)Cl₂] reacts with salmon sperm DNA, two GpG adducts are also observed, and following enzymatic digestion,

(45) Admiraal, G.; van der Veer, J. L.; de Graaff, R. A. G.; den Hartog, J. H. J.; Reedijk, J. *J. Am. Chem. Soc.* **1987**, *109*, 592–594.

these adducts comigrate with bands I and II.²² However, they are not observed in equal proportions, band II predominating over band I by a factor of 3.3:1. This difference between the proportions of bands I and II obtained in the reaction with the dinucleotide and that obtained in the reaction with salmon sperm DNA is not surprising given the reduced conformational freedom in duplex DNA and the consequently increased likelihood of steric interactions between the hpip ligand and the DNA having an influence on the population of each isomer. The present study has allowed us to assign the two isomers and so address the reasons for the stereoselectivity of the reaction with duplex DNA represented by the increased proportion of band II. The two sites of [Pt(hpip)Cl₂] available for reaction with DNA are enantiomerically related, and therefore, a preference for reaction with either the 5' or the 3' side of the GpG pair might contribute to the stereoselectivity. However, this is likely to be a minor factor, and we suggest that the stereoselectivity arises from the differences among the interactions that

occur between the DNA and either the two carbon or three-carbon links. We have shown elsewhere that interactions between amine ligands and the exocyclic group (O or NH₂) in the 6 position of the 3' guanine or adenine of a GpG, ApG, or GpA site probably have an influence on the likelihood of reaction at such a site.¹⁷ The propylene link is undoubtedly bulkier and therefore can be expected to make closer and more unfavorable interactions with the exocyclic oxygen atom of the 3' guanine in a GpG pair. This proposal is consistent with the preference for band II since it has the ethylene link disposed toward this exocyclic oxygen atom and is supported by molecular mechanics calculations that we present elsewhere.²²

Acknowledgment. We thank the Sydney University Cancer Research Fund and the Australian Research Council for financial support.

IC951489D